PAPER

Controlled surface oxidation of multi-layered graphene anode to increase hole injection efficiency in organic electronic devices

2D Materials

RECEIVED
29 June 2015

REVISED
13 November 2015

ACCEPTED FOR PUBLICATION
4 December 2015

PUBLISHED
18 January 2016

PAPER

Controlled surface oxidation of multi-layered graphene anode to increase hole injection efficiency in organic electronic devices

Tae-Hee Han[1], **Sung-Joo Kwon**[1], **Hong-Kyu Seo and Tae-Woo Lee**

Department of Materials Science and Engineering, Pohang University of Science and Technology (POSTECH), 77 Cheongam-Ro, Nam-Gu, Pohang, Gyungbuk 790-784, Korea

[1] These authors contributed equally to this work

E-mail: twlee@postech.ac.kr **and** taewlees@gmail.com

Keywords: graphene, hole injection, graphene oxide, surface treatment

Abstract

Ultraviolet ozone (UVO) surface treatment of graphene changes its sp^2-hybridized carbons to sp^3-bonded carbons, and introduces oxygen-containing components. Oxidized graphene has a finite energy band gap, so UVO modification of the surface of a four-layered graphene anode increases its surface ionization potential up to ~5.2 eV and improves the hole injection efficiency (η) in organic electronic devices by reducing the energy barrier between the graphene anode and overlying organic layers. By controlling the conditions of the UVO treatment, the electrical properties of the graphene can be tuned to improve η. This controlled surface modification of the graphene will provide a way to achieve efficient and stable flexible displays and solid-state lighting.

1. Introduction

Graphene has a linear energy momentum dispersion with a zero gap at the Dirac point, so electrons in the graphene behave as massless quasi-particles with high charge carrier mobility [1–5]. Graphene's electrical properties have been applied in various areas of electronics such as transistors, memories and interconnects [4–8]. However, graphene has no band gap, and is therefore not suitable for use in logic and switching devices that require a finite band gap. To overcome this limitation of pristine graphene, several authors have attempted to induce a band gap in it [9–15]. Oxygen plasma treatment (OPT) has often been used to modify graphene to make it applicable in switching devices [16–18]. Simple OPT introduces covalently-bonded oxygen atoms, which oxidize graphene to many forms, including carbonyl (CO), hydroxyl (OH) and epoxide (COC) groups, and aggressively break the sp^2-hybridized carbon atomic ordering of pristine graphene. Consequently, OPT significantly degrades the linear energy momentum dispersion of pristine graphene, and thereby reducing the electrical conductivity of the graphene and opening a finite energy band gap [16–18]. The excellent mechanical properties and high optical transparency (*OT*) of graphene make it a candidate for use as a flexible transparent conducting electrode that can replace the brittle indium-tin-oxide (ITO) electrode to enable development of flexible optoelectronic devices [19–24]. However, the relatively low work function (*WF*) of pristine graphene (~4.3–4.5 eV) compared to that of ITO (~4.7–4.9 eV) limits hole injection to overlying organic layers (e.g. highest occupied molecular orbital (HOMO) of N,N′-Bis(naphthalen-1-yl)-N,N′-bis(phenyl)benzidine (NPB) ~5.4 eV) from a graphene anode due to formation of a large energy barrier at the interface in organic light-emitting diodes (OLEDs) [23]. Inefficient carrier injection from electrodes severely diminishes luminous efficiency and device stability due to its unbalanced charge injection and recombination of holes and electrons in OLEDs. Although hole injection layers (HILs) made from conducting polymers such as poly (3,4-ethylenedioxythiphene):poly-(styrenesulfonate) (PEDOT:PSS) have been conventionally used to enhance the hole injection from the anode, the *WF* difference between the graphene anode (~4.4 eV) and the PEDOT:PSS HIL (~5.2 eV) remains too large to allow easy hole injection [25]. One possible way to reduce the graphene anode's large energy barrier for hole injection is to open the energy band gap to provide an intermediate step for hole injection. Graphene oxide and reduced graphene oxide films have been used as hole injection or extraction layers to reduce the

energy barrier between the anode and the organic layer in organic electronics [26–30]. These films are composed of graphene oxide flakes, so it is difficult to make full-coverage film, and the film surface can be rough; this trait can severely degrade device reliability and increase sample-to-sample variation [28–30]. In addition, films that consist of graphene oxide or reduced graphene oxide are covered by many functional groups, which degrade its electrical properties, so it is not suitable for use as an electrode due to high sheet resistance [30–32]. Using a high-quality single-layer graphene (SLG) or a multi-layered graphene film grown by using chemical vapor deposition (CVD) can be an alternative method to provide a smooth surface and low sheet resistance as electrodes in OLEDs [20, 21, 23, 24]. However, because plasma treatment or ion irradiation easily convert the graphene into an insulating graphene oxide due to aggressive plasma and ion bombardment, these kinds of high-energy treatments are not suitable for the production of graphene anodes for OLEDs [16, 17, 33]. Controlled gentle ultraviolet ozone (UVO) treatment can tune the electrical properties of the graphene. Surface-modified graphene by surface treatment processes to make a hydrophilic surface is also essentially required to deposit a polymeric HIL on the graphene anode because water-based polymeric HILs on the pristine graphene cannot be deposited uniformly due to their hydrophobicity [34, 35]. Therefore, if UVO treatment is to be used to achieve high-efficiency flexible OLEDs with a graphene anode, the effects of this treatment on hole injection from the graphene anode must be understood. Here, we report the preparation of graphene anodes by the UVO surface treatment, and demonstrate that this treatment increases hole injection from the multi-layered graphene anode. The influences of the UVO treatment on graphene were analyzed systematically in SLG grown using CVD and in four-layer graphene (4LG) formed by stacking four SLGs. We also fabricated single carrier devices that have 4LG anodes, and studied the effect of UVO treatment duration (T) on hole injection capability from the graphene anode.

2. Materials and methods

2.1. Fabrication of SLG and 4LG

Graphene films were synthesized using CVD growth on Cu foil (25 μm thickness, Alfa Aesar). Cu foils were placed in the center of a quartz tube in a furnace and were heated to 1060 °C, then annealed at that temperature for 30 min in a flow of 15 sccm of H_2. As a carbon precursor for graphene, 60 sccm of CH_4 gas was passed through the tube for 30 min, then the Cu foils were cooled rapidly to room temperature. Poly(methyl methacrylate) (PMMA) solution dissolved in chlorobenzene (4.6 g/100 ml) was spin-coated on top of the graphene as a supporting polymer during the transfer process. Before etching Cu foil, graphene grown on the bottom side of the Cu foil was etched away using a reactive ion etcher (RIE) at 100 W for 10 s in O_2 gas at a pressure of 200 mTorr. The Cu foil was etched using $FeCl_3$-based Cu etchant, CE-100 (Transene). Etchant residue of SLG/PMMA was rinsed off by floating in deionized water twice. The SLG sheet was transferred onto a glass substrate. The PMMA layer was removed by soaking the graphene/PMMA in an acetone bath. To obtain 4LG sheets, the transfer processes of SLG were repeated four times. The SLG and 4LG were surface-treated using a UVO cleaner (AH1700 from AHTECH LTS, UV light intensity: 28 mW cm^{-2}, distance from sample to lamp: 25 mm) for various T.

2.2. Characterization of graphene and devices

The sheet resistance and transmittance of SLG and 4LG were measured using a four-point probe with a Keithley 2400 and UV–vis spectrometer (SCINCO S-3100), respectively. Raman spectra were measured using a 532-nm laser source (WITEC). The potential changes of the graphene surface were measured using a Kelvin probe (SKP-5050). X-ray photoelectron spectroscopy (XPS) was performed using a Theta Probe AR-XPS System (Thermo Fisher Scientific, UK), with monochromated Al-Ka as the x-ray source (1486.6 eV).

A pre-patterned ITO anode on a glass substrate was sonicated with acetone and isopropyl alcohol in an ultrasonic bath and then boiled on a hot plate to remove any contaminants on the glass substrate. SLGs were transferred onto the cleaned pre-patterned ITOs and 4LGs were transferred onto PET substrate. The SLG/pre-patterned ITO and 4LG/PET were UVO-treated for various T. For the hole-only devices (HODs) that used a 4LG anode, a 50-nm-thick polymeric gradient hole injection layer (GraHIL) composed of PEDOT:PSS (AI4083) and perfluorinated ionomer (1:3.6, w:w) was spin-cast on top of the 4LG anode. Then a 500-nm-thick (HODs with SLG) or 2.27-μm-thick (HODs with 4LG) NPB and a 110-nm-thick aluminum cathode were deposited using a thermal evaporator in a high vacuum ($<5 \times 10^{-7}$ Torr). The fabricated devices were encapsulated by a glass lid and UV-curable epoxy resin. The current density–voltage characteristics of HODs were measured using a Keithley 236 source meter.

3. Results and discussion

SLG grown using CVD and transferred on the PET or the glass substrate had $OT > 97\%$ at 550 nm; this is close to the theoretical value [20, 21]. The 4LG fabricated by stacking SLGs on the substrate maintains $OT \sim 90\%$. Because OT is reduced by ~2.3% per graphene layer theoretically, the OT results indicate that the graphene was of high quality and that this successive stacking process successfully fabricated a

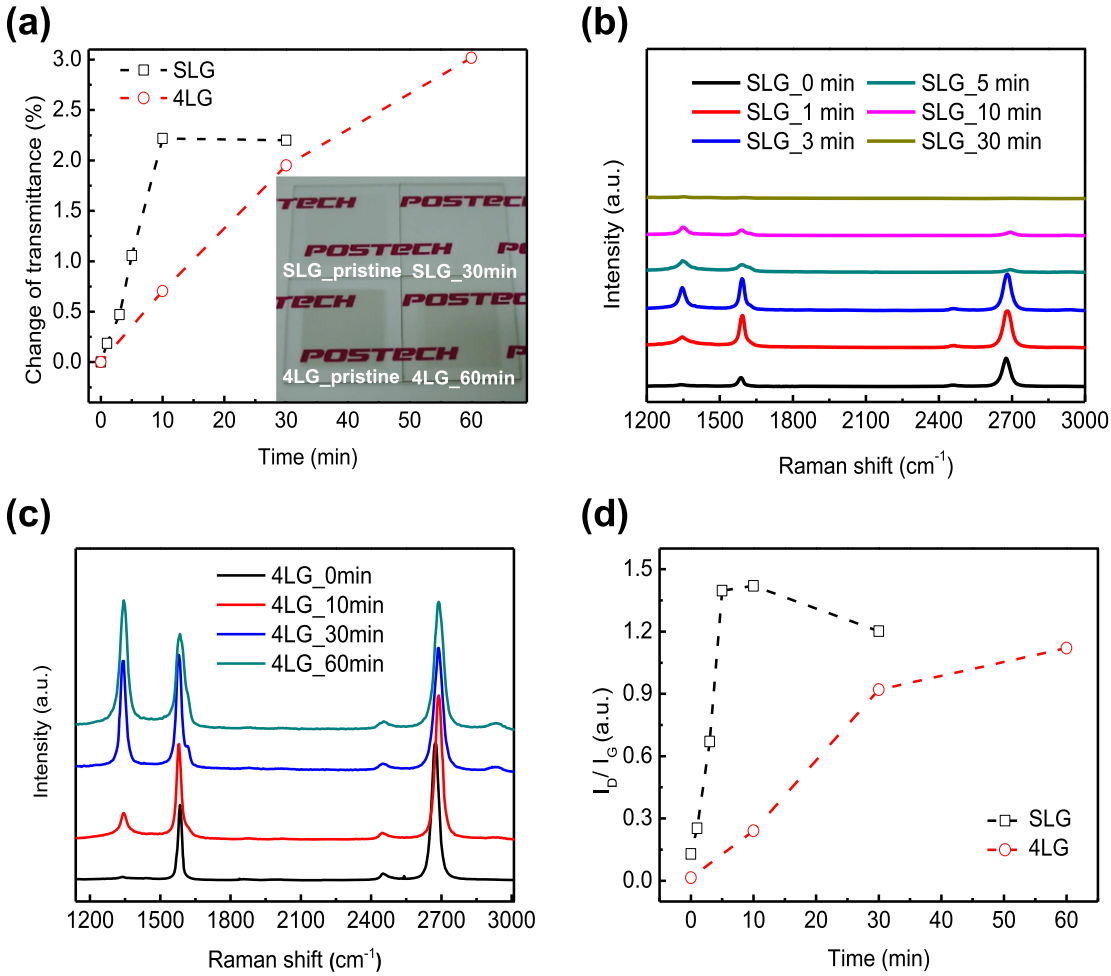

Figure 1. (a) Change of optical transmittance with varying UVO treatment times in SLG and 4LG. Raman spectra of (b) pristine SLG and UVO-treated SLG, (c) pristine 4LG and UVO-treated 4LG, (d) intensity ratio of D to G band in Raman spectroscopy with varying UVO treatment times in SLG and 4LG.

multi-layered graphene anode. In SLGs, *OT* increased rapidly with the increase in UVO treatment $0 \leqslant T \leqslant 10$ min (total increase ~2.2%), but did not increase further at $10 < T \leqslant 30$ min. In 4LG, *OT* increased continuously from ~90% at $T = 0$ to 92.6% at $T = 60$ min (figure 1(a)). The increase in *OT* is related to the degree of graphene oxidation, which is related to the increase in sp^3 amorphous carbons and structural defects induced by surface treatment [36, 37].

The growth of high-quality SLG and fabrication of 4LG were also analyzed and confirmed using average Raman spectroscopy of large areas ($50 \times 50\ \mu$m) of the graphene surface (figures 1(b), (c)). In the SLG, the peak intensity ratio of the 2D band (~2676 cm^{-1}) to the G band (~1587 cm^{-1}) was ~3.25, and that of the D band (~1350 cm^{-1}) to the G band was ~0.1; these results mean that the SLG was near one atom thick with few structural defects. In 4LG, the peak intensity ratio of the 2D to G band decreased to ~1.8 due to local interactions between SLGs [38, 39]. The ratio of its D to G band was very low (~0.01); this also indicates that the stacking of SLGs to fabricate 4LG did not cause additional structural defects on the graphene anode. The G band represents the planar sp^2 carbon lattice and the D band is closely related to defects or disorder in the graphene, and the intensity ratio of the D to G band can be a direct indicator of the ratio of non-sp^2 bonded carbons to sp^2-bonded carbons [16, 17, 40, 41]. In the SLG, the intensities of these bands in the graphene gradually decreased as *T* increased, and at $T = 30$ min, they were indistinct and showed very low intensities. The intensity ratio of the D to G band rapidly increased until $T = 5$ min (~1.40), then increased slightly more at $T = 10$ min (~1.42) (figures 1(b) and (d)), but after $T = 30$ min the D to G band intensity ratio decreased (~1.20). These results can be attributed to the saturation of the oxidation level after $T = 10$ min and the expulsion of oxygen species by additional exposure to UV light [41]. The 4LG also showed a gradual increase in the intensity ratio of the D to G band as *T* increased, but the intensities of characteristic bands were not significantly reduced as *T* increased. Furthermore, at $T = 10$ min, UVO-treated 4LG exhibited a much lower intensity ratio of the D to G band (~0.24) than

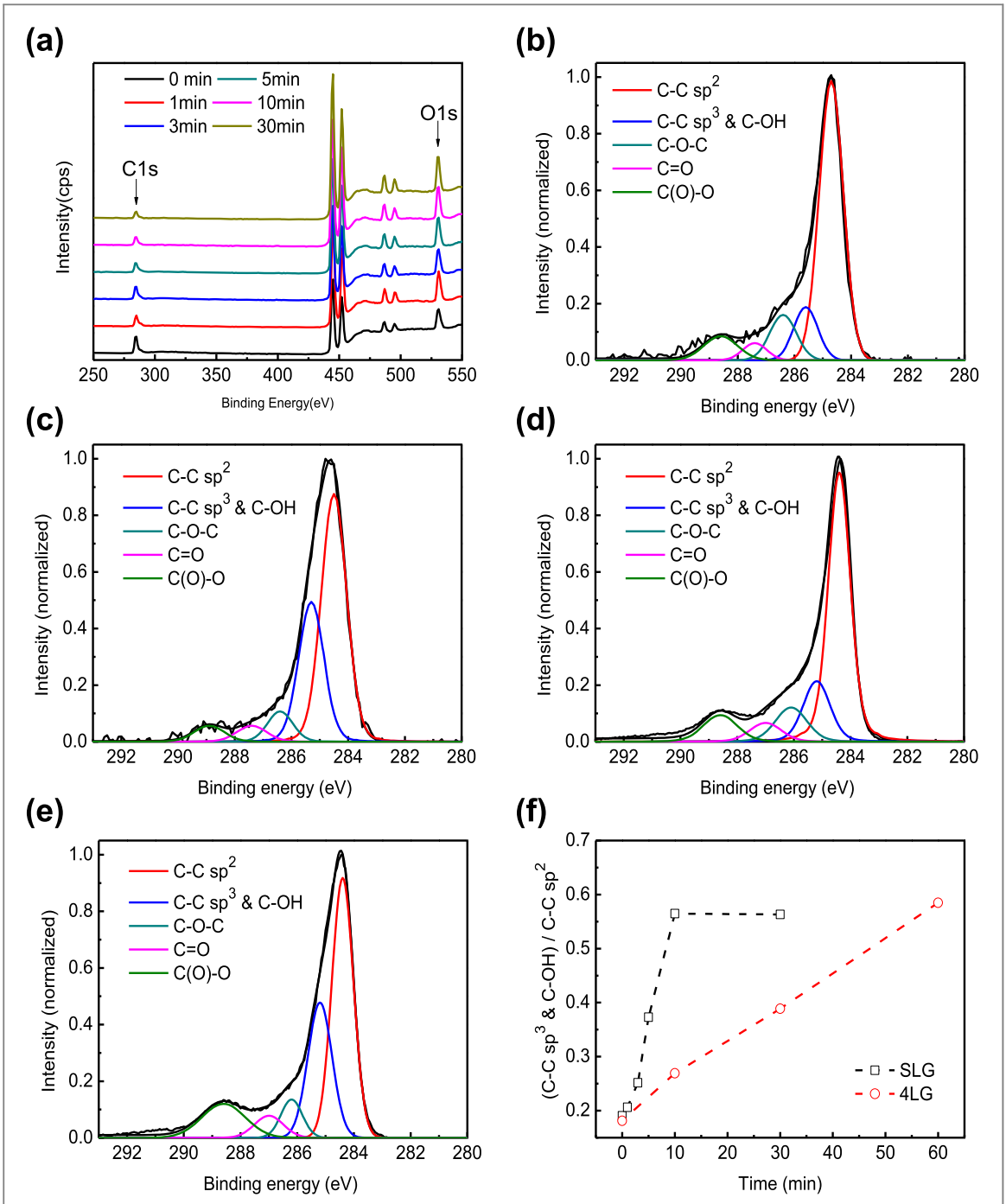

Figure 2. (a) XPS survey spectra of pristine SLG and UVO-treated SLG. Deconvoluted XPS C1s spectra of (b) pristine SLG, (c) SLG treated with UVO for 10 min, (d) 4LG treated using UVO for 10 min and (e) 4LG treated using UVO for 60 min. (f) Deconvoluted area ratios of sp^3 C-C and C-OH (~285.5 eV) to sp^2 C-C (~284.5 eV).

SLG (~1.4), and the ratio gradually increased even until $T = 60$ min (figures 1(c) and (d)).

To identify the change of chemical components in the graphene under UVO treatment, we also performed XPS analysis of SLG and 4LG (figure 2). The XPS survey spectra of SLG (figure 2(a)) clearly showed a gradual increase in oxygen compounds and a gradual decrease in carbon compounds as T increased. Deconvolution of C1s core level spectra of graphene revealed sp^2 C-C bonding (~284.5 eV) and four different oxygen-containing components including non-sp^2-bonded C-C or C-OH (~285.6 eV), C-O-C (~286.4 eV), C=O (~287.4 eV) and C(O)O (~288.6 eV) in both SLG and 4LG (figures 2(b)–(e)) [42–44]. In pristine SLG, deconvoluted peaks demonstrate that oxygen compounds were significantly lower than those of sp^2-hybridized carbon bonds (figure 2(b)). The C1s spectrum of the 10 min UVO-treated SLG clearly showed a distinct increase in a peak representing non-sp^2-bonded carbons and the C-OH (~285.5 eV) in the XPS (figure 2(c)). In SLG, the ratio of areas under the deconvoluted peaks of non-sp^2-bonded carbons and C-OH to sp^2-hybridized carbons drastically increased until $T = 10$ min, then reached an asymptote

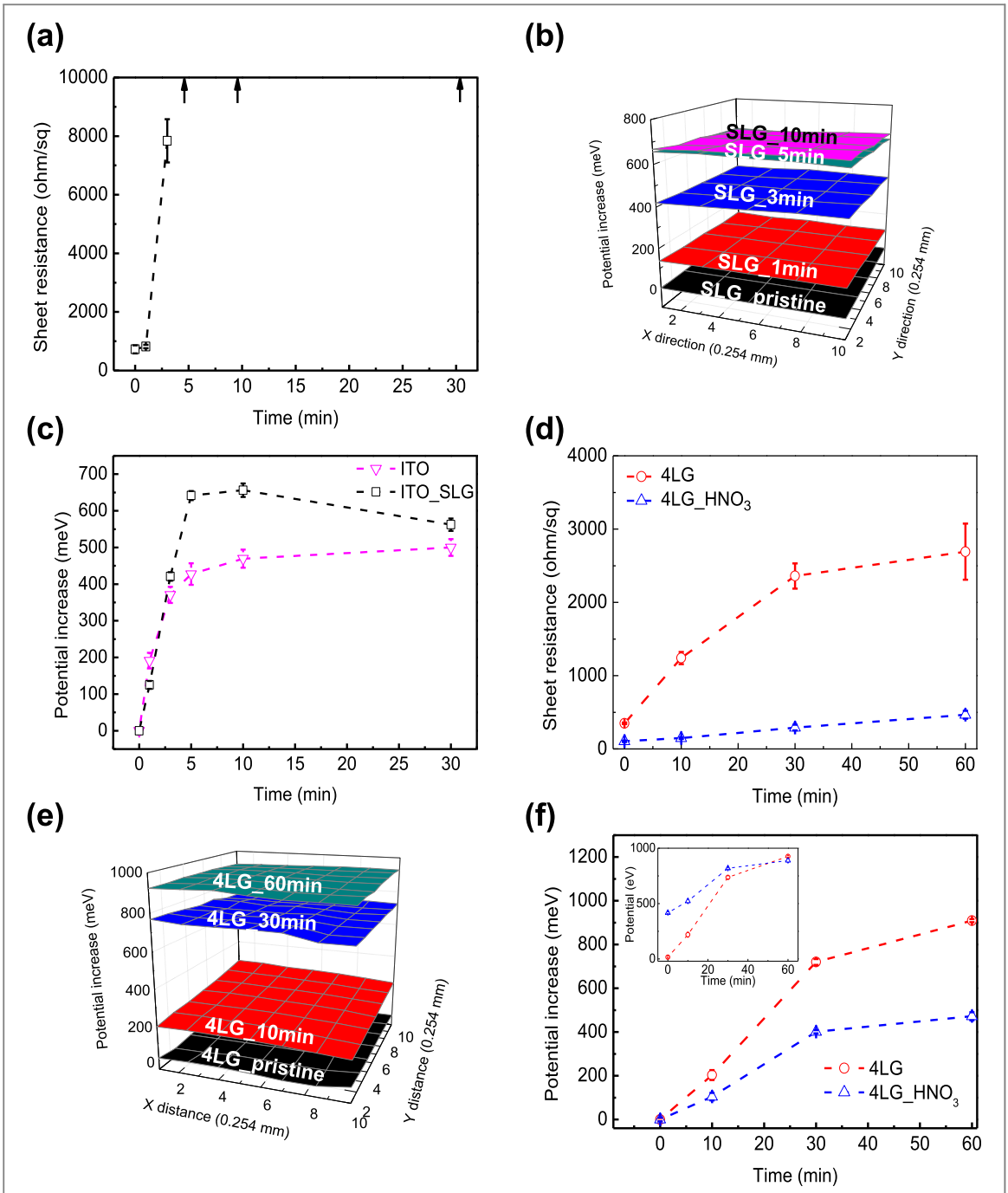

Figure 3. (a) Sheet resistances R_S of pristine SLG and UVO-treated SLG; (b) potential increase mapping of SLG; (c) potential increase of ITO and ITO/SLG with varying UVO treatment times; (d) R_S of 4LG and HNO_3-doped 4LG; (e) potential increase mapping of 4LG; (f) potential increase of 4LG and HNO_3-doped 4LG with varying UVO treatment times. (inset: surface ionization potential of 4LGs and HNO_3-doped 4LGs).

(figure 2(f)). We can note that the overtaking of oxygen-related peaks which have high binding energies in C1s did not occur, as has been observed in graphene oxide made using other methods [18, 29–31]; this result shows that the mild conditions of UVO treatment provide the ability to control graphene oxidation. In 4LG, the UVO treatment resulted in similar changes (prominent increase of non-sp^2-bonded carbons or C-OH) to those in SLG (figures 2(d) and (e)); the XPS spectrum of 4LG at $T = 10$ min showed a much smaller peak at 285.5 eV (ratio ~0.27) than that of SLG (~0.57) (figure 2(f)). Furthermore, as T increased, the ratio between the two deconvoluted peaks increased gradually and continuously until $T = 60$ min in 4LG (figures 2(e) and (f)). These results of the *OT*, Raman spectroscopy and XPS indicated that (i) SLGs are rapidly oxidized under UVO treatment until $T = 10$ min and oxidation does not increase at $T > 10$ min; (ii) overexposure to UV light ($T = 30$ min) can expel residual graphene oxide from the substrate; (iii) 4LG oxidized much more slowly than SLG. These results mean that the top layer of 4LG

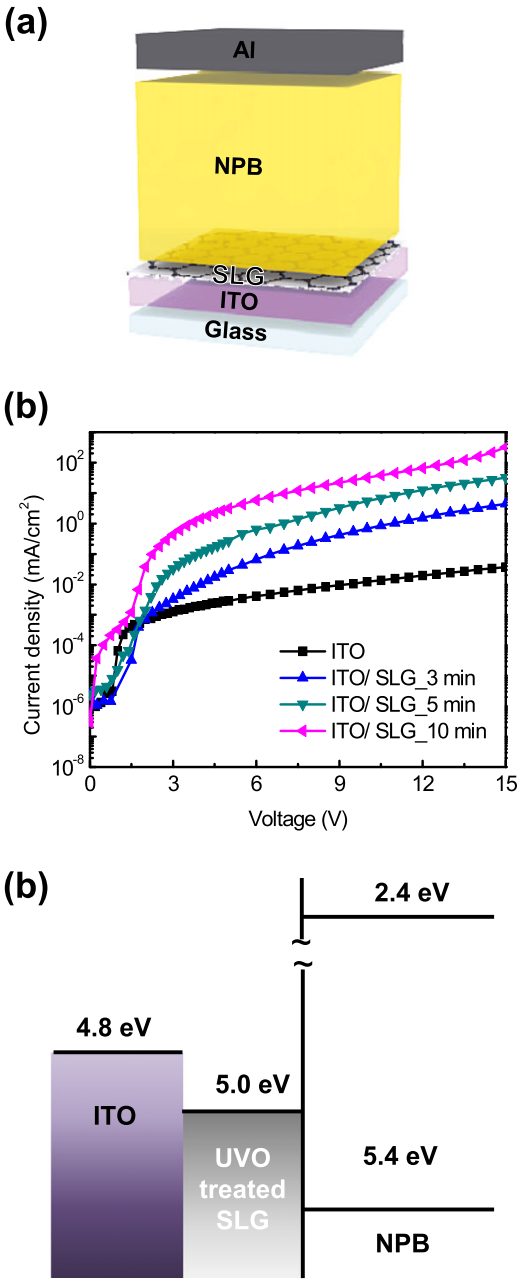

Figure 4. (a) Schematic illustration of a HOD structure using SLG; (b) hole current density according to applied voltages; (c) schematic energy band diagram for HOD using 10 min UVO-treated SLG as HIL.

effectively protects layers below it from oxidation by UVO because oxidation of multi-layered graphene by surface treatment occurs layer by layer [16, 17].

To identify the influences of UVO treatment on the electrical properties of graphene, we measured the sheet resistance (R_S) and the change of surface potential (figure 3). In SLG, the initial R_S (~724.2 Ω sq^{-1}) did not change much after $T = 1$ min ($R_S \approx 818.9$ Ω sq^{-1}), but increased rapidly to ~7,840 Ω sq^{-1} at $T = 3$ min (figure 3(a)) and exceeded the measurement range of the four-point probe measurement device at $T \geqslant 5$ min. ITO anodes are often treated using UVO to make their surface hydrophilic by introducing hydroxyl (-OH), carbonyl (-CO) or carboxyl (-COOH) groups and to increase the anodes' surface *WF* [45]. In our experimental results, the surface potential of the ITO increased continuously but reached an asymptote after $T = 10$ min (figures 3(b) and (c)). The surface potential of SLG on the glass/ITO substrate increased more rapidly and by a greater amount (~656.3 meV) until $T = 10$ min than that of ITO (~469.4 meV) (figures 3(b) and (c)). However, after $T = 30$ min the surface potential of SLG decreased slightly (~562.3 meV) compared with that after $T = 10$ min (figure 3(c)). Electrical properties of SLG treated using UVO indicate that it rapidly oxidizes the SLG and changes semi-metallic SLG to an insulator after treatment for $T < 10$ min. UVO treatment breaks the pristine atomic ordering by changing the sp^2-bonded carbon network of graphene to sp^3 carbons and oxygen-containing graphene oxide, and thereby strongly affects graphene's electronic band structure and ultimately opens an energy band gap, increasing ionization potential as T increases [16, 17, 46]. In 4LG, R_S also increased gradually as T increased, but the increase in R_S was much lower than in SLG. After $T = 10$ min, the R_S of 4LG was about three times (~1240.2 Ω sq^{-1}) that of pristine 4LG (~349.9 Ω sq^{-1}), and continuously increased until $T = 60$ min (~2692.0 Ω sq^{-1}) (figure 3(d)). At the same time, the surface potential also significantly increased by ~909.3 meV at $T = 60$ min from that of the pristine 4LG (figures 3(e) and (f)). When we used HNO_3 to chemically dope 4LG to increase its electrical conductivity, R_S decreased to 104.2 Ω sq^{-1}. Furthermore, UVO treatment of HNO_3-doped 4LG did not cause a significant increase in R_S (~465.9 Ω sq^{-1} at $T = 60$ min) (figure 3(d)). Although the amount of the surface potential increase in the HNO_3-doped 4LG was also reduced (~472.1 meV increase at $T = 60$ min), the final surface ionization potential value of the HNO_3-doped 4LG treated for $T = 60$ min (~5.2 eV) was similar to that of undoped 4LG due to the p-type doping effect of graphene by HNO_3 (figures 3(e) and (f)). These results indicate that appropriate combination of the UVO treatment and chemical doping can yield a 4LG anode that has both an appropriate R_S ~465.9 Ω sq^{-1} and greatly enhanced surface *WF* ~ 5.2 eV.

To prove that the UVO treatment enhances hole injection on the graphene, we fabricated HODs that had ITO/SLG or 4LG anodes (figure 4(a)). Because the UVO-treated SLG has a very high R_S and is a near-insulator, the increased surface potential of SLG on ITO by UVO treatment (~0.2 eV) can facilitate hole injection between the ITO anode and hole transporting layer (HTL). The surface *WF* of UVO-treated ITO is ~4.8 eV [45], so UVO-treated SLG can provide an effective intermediate state between ITO and HTL (e.g., HOMO of NPB ~5.4 eV). When we fabricated HODs [ITO/SLG/NPB (500 nm)/Al (110 nm)] using SLG treated with UVO for $T = 3$, 5 or 10 min (figure 4(a)), the current densities (J) of HODs

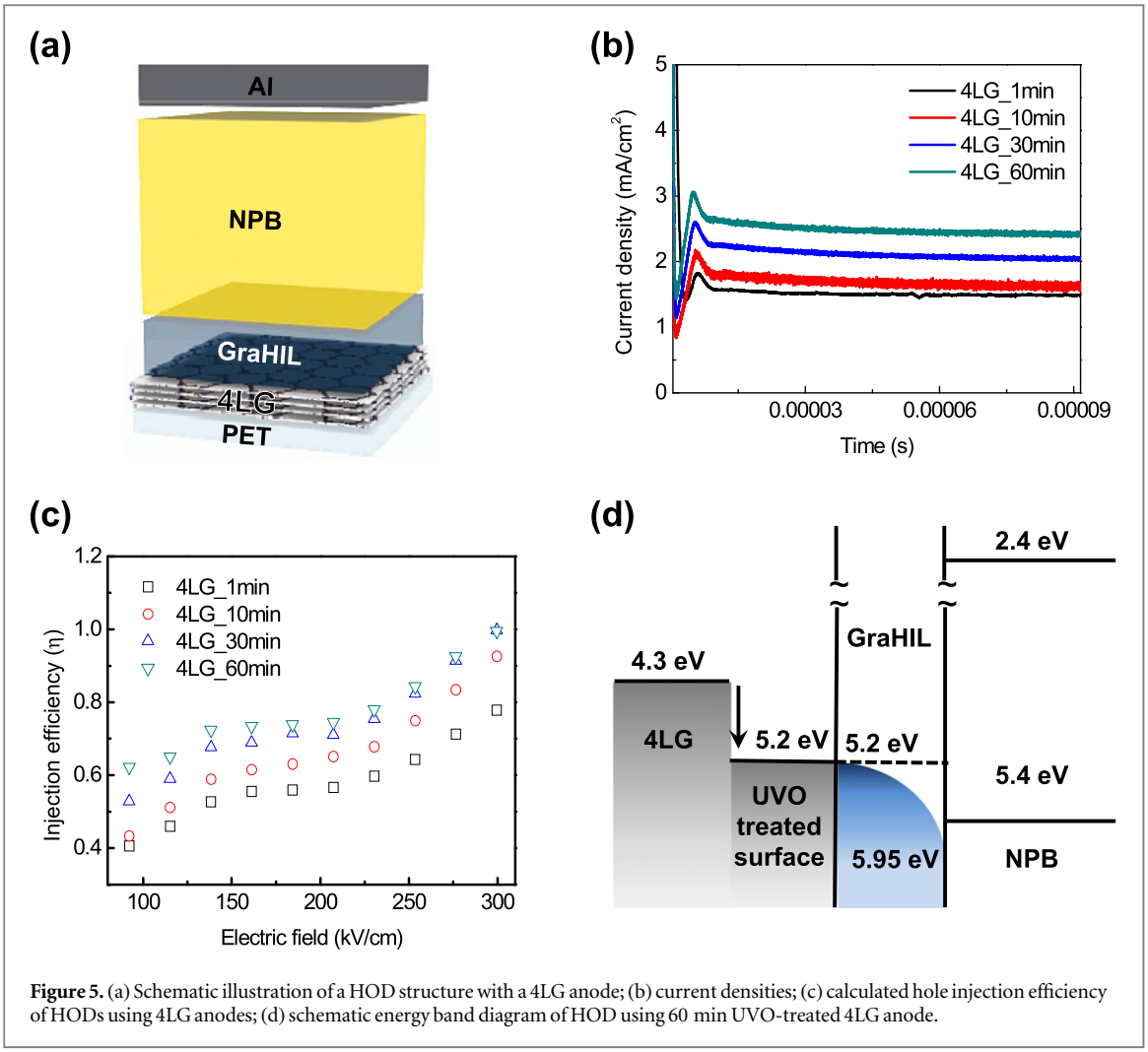

Figure 5. (a) Schematic illustration of a HOD structure with a 4LG anode; (b) current densities; (c) calculated hole injection efficiency of HODs using 4LG anodes; (d) schematic energy band diagram of HOD using 60 min UVO-treated 4LG anode.

gradually increased according to the tendency of surface ionization potential increase of SLG on ITO under UVO treatment (figure 4(b)). Because the UVO treatment of SLG on the ITO anode additionally provides intermediate states for hole injection between the ITO anode and the NPB, the SLG for $T = 10$ min (~5.0 eV) on the ITO anode yielded the HOD with the highest J (figures 4(b) and (c)). To observe the capability for hole injection from the graphene anode, we also fabricated HODs that had UVO-treated 4LG anodes, then used them in transient measurements of dark-injection space-charge-limited-current (DI-SCLC) [4LG/GraHIL (~50 nm)/NPB (2.27 um)/Al (110 nm)] (figure 5(a)). To clearly observe the DI peak that is observed when ohmic contact is formed at the carrier-injecting interface, we also used a polymeric HIL (GraHIL), which develops a gradually increasing *WF* by self-organization between the graphene anode and the NPB layer [23, 47–49]. To avoid the coating issue of water-based PEDOT:PSS on the hydrophobic pristine graphene surface, we used 4LG treated using UVO for $T = 1$ min instead of pristine 4LG. By comparing the *J*s of HODs with theoretical SCLC, we can calculate the carrier injection efficiency (η) of hole-injecting contact between the graphene anode and overlying organic layer (i.e. NPB) as

$$\eta = \frac{J_{\text{peak}}}{1.2 \times J_{\text{SCL}}}, \tag{1}$$

where J_{peak} is J at the DI peak and

$$J_{\text{SCL}} = \frac{9}{8}\epsilon\epsilon_0\mu_0 \exp(\beta\sqrt{E})\frac{E^2}{d} \tag{2}$$

is the theoretical SCLC, where ε is the dielectric constant, ε_0 is the vacuum permittivity, μ_0 is the zero-field mobility, β is the Pool–Frenkel constant, E is the electric field and d is the film thickness. When we measured the *J*s of HODs by applying a 20 V square voltage pulse, J increased as T on the 4LG increased (figure 5(b)). Consequently, η increased gradually as the surface of the 4LG anode was modified by UVO treatment to have high surface ionization potential (figure 5(c)). Furthermore, η was close to 1, which is the ideal value; $\eta = 1$ means that ideal ohmic contact is formed. As T on the 4LG increased, the breakup of the sp^2 carbon network by introducing oxygen atoms on the 4LG surface severely changed graphene's electrical band structure. The increase in surface ionization potential resulting from the band gap opening of the modified 4LG surface removes the energy barrier to hole injection between the graphene anode

and HIL (figure 5(d)). As a result, 4LG treated with 60 min UVO had a nearly negligible hole injection energy barrier, so η calculated from DI-SCLC indicated near-perfect ohmic contact between the graphene and overlying layers.

4. Conclusion

We conducted studies to identify the effects of UVO treatment on the physical, chemical and electrical properties of SLG synthesized by CVD and of 4LG formed by stacking SLGs. We tried to provide tunable electronic and electrical properties of the graphene by applying mild UVO treatment. SLG was rapidly changed into an insulator by oxidation and reached saturated oxidation level after UVO treatment for duration $T = 10$ min. 4LG showed a much slower oxidation because the top SLG layer in the 4LG protects the graphene under it from UVO treatment. The optical transmittance, Raman spectroscopy, XPS, sheet resistance and Kelvin probe showed similar tendencies as T increased. UVO treatment disturbs sp^2-hybridized carbon ordering of pristine graphene by introducing oxygen-containing groups on the graphene. Because the increased components of non-sp^2-bonded carbons and oxygen-containing groups in the graphene change the electronic band structure of π-networks in the graphene, UVO treatment causes the creation of a finite band gap and increases surface ionization potential in the graphene. As a result, UVO treatment for 10 min increased the surface ionization potential of SLG on ITO (~5.0 eV); therefore, UVO-treated SLGs can be used as HILs to increase hole injection between the ITO anode (~4.8 eV) and the HTL. UVO treatment for 60 min modified the 4LG surface to give it a high surface ionization potential. Furthermore, additional chemical p-type doping greatly reduced sheet resistance ($R_S \sim 465.9\ \Omega\ sq^{-1}$) of the graphene anode while maintaining its high surface ionization potential (~5.2 eV). We confirmed that UVO treatment of 4LG can improve its hole injection efficiency by reducing the energy barrier between the anode and the overlying layer. This study proves the influence of UVO treatment on the electronic and electrical properties of graphene, and suggests the importance of well-controlled surface treatment of graphene anodes to enhance hole injection. This kind of suitable surface treatment of the graphene anode before fabricating devices can be used to improve the electrical properties of optoelectronic devices that use graphene anodes.

Acknowledgements

This work was supported by the National Research Foundation of Korea (NRF) grant funded by the Korea government (NRF-2013R1A2A2A01068753) and the MSIP (Ministry of Science, ICT and Future Planning), Korea, under the "ICT Consilience Creative Program" (IITP-2015-R0346-15-1007) supervised by the IITP (Institute for Information & communications Technology Promotion).

References

[1] Novoselov K S, Geim A K, Morozov S V, Jiang D, Zhang Y, Dubonos S V, Grigorieva I V and Firsov A A 2004 *Science* **306** 666
[2] Novoeslov K S, Geim A K, Morozov S V, Jiang D, Katsnelson M I, Grigorieva I V, Dubonos S V and Firsov A A 2005 *Nature* **438** 197
[3] Zhang Y, Tan Y, Stormer H L and Kim P 2005 *Nature* **438** 201
[4] Rogers J A 2008 *Nature Nanotech.* **3** 254
[5] Novoselov K S, Falko V I, Colombo L, Gellert P R, Schwab M G and Kim K 2012 *Nature* **490** 192
[6] Hong A J *et al* 2011 *ACS Nano* **5** 7812
[7] Song E B *et al* 2011 *Appl. Phys. Lett.* **99** 042109
[8] Chen X, Akinwande D, Lee K-J, Close G F, Yasuda S, Paul B C, Fujita S, Kong J and Wong H-S P 2010 *IEEE Trans. Electron Devices* **57** 3137
[9] Han M Y, Ozyilmaz B, Zhang Y and Kim P 2007 *Phys. Rev. Lett.* **98** 206805
[10] Jia X *et al* 2009 *Science* **323** 1701
[11] Li X, Wang X, Zhang L, Lee S and Dai H 2008 *Science* **319** 1229
[12] Wu X, Sprinkle M, Li X, Ming F, Berger C and Heer W A 2008 *Phys. Rev. Lett.* **101** 026801
[13] Yan J-A, Xian L and Chou M Y 2009 *Phys. Rev. Lett.* **103** 086802
[14] Elias D C *et al* 2009 *Science* **323** 610
[15] Xu W, Seo H-K, Min S-Y, Cho H, Lim T-S, Oh C-Y, Lee Y and Lee T-W 2014 *Adv. Mater.* **26** 3459
[16] Nourbakhsh A, Cantoro M, Vosch T, Pourtois G, Clemente F, Veen M H, Hofkens J, Heyns M M, Gendt S D and Sels B F 2010 *Nanotechnology* **21** 435203
[17] Gokus T, Nair R R, Bonetti A, Bohmler M, Lombardo A, Novoselov K S, Geim A K, Ferrari A C and Hartschuh A 2009 *ACS Nano* **3** 3963
[18] Felten A, Eckmann A, Pireaux J-J, Krupke R and Casiraghi C 2013 Controlled modification of mono- and bilayer graphene in O2, H2 and CF4 plasmas *Nanotechnology* **24** 355705
[19] Kumar A and Zhou C 2010 *ACS Nano* **4** 11
[20] Kim K S, Zhao Y, Jang H, Lee S Y, Kim J M, Kim K S, Ahn J-H, Kim P, Choi J-Y and Hong B H 2009 *Nature* **457** 706
[21] Bae S *et al* 2010 *Nature Nanotech.* **5** 574
[22] Bonaccorso F, Sun Z, Hasan T and Ferrari A C 2010 *Nature Photon.* **4** 611
[23] Han T-H, Lee Y, Choi M-R, Woo S-H, Bae S-H, Hong B H, Ahn J-H and Lee T-W 2012 *Nature Photon.* **6** 105
[24] Kim H, Bae S-H, Han T-H, Lim K-G, Ahn J-H and Lee T-W 2014 *Nanotechnology* **25** 014012
[25] Lee T-W and Chung Y 2008 *Adv. Funct. Mater.* **18** 2246
[26] Li S-S, Tu K-H, Lin C-C, Chen C-W and Chhowalla M 2010 *ACS Nano* **4** 3169
[27] Liu J, Xue Y, Gao Y, Yu D, Durstock M and Dai L 2012 *Adv. Mater.* **24** 2228
[28] Lee B R, Kim J-W, Kang D, Lee D W, Ko S-J, Lee H J, Lee C-L, Kim J Y, Shin H S and Song M H 2012 *ACS Nano* **6** 2984
[29] Shi S, Sadhu V, Moubah R, Schmerber G, Bao Q and Silva S R P 2013 *J. Mater. Chem.* C **1** 1708
[30] Liu J, Durstock M and Dai L 2014 *Energy Environ. Sci.* **7** 1297
[31] Dreyer D R, Park S, Bielawski C W and Ruoff R S 2010 *Chem. Soc. Rev.* **39** 228
[32] Loh K P, Bao Q, Eda G and Chhowalla M 2010 *Nature Chem.* **2** 1015
[33] Chen J-H, Cullen W G, Jang C, Fuhrer M S and Williams E D 2009 *Phys. Rev. Lett.* **102** 236805
[34] Park H, Howden R M, Barr M C, Bulovic V, Gleason K and Kong J 2012 *ACS Nano* **6** 6370
[35] Park H, Chang S, Smith M, Gradečak S and Kong J 2013 *Sci. Rep.* **3** 1581

[36] Lu Z-B, Zhao X, Zhang X-L, Yan X-Q, Wu Y-P, Chen Y-S and Tian J-G 2011 *J. Phys. Chem. Lett.* **2** 1972–7
[37] Wang L *et al* 2015 *Light Sci. Appl.* **4** e253
[38] Das A *et al* 2008 *Nature Nanotech.* **3** 210–5
[39] Casiraghi C 2009 *Phys. Rev.* B **80** 233407
[40] Ferrari A C *et al* 2006 *Phys. Rev. Lett.* **97** 187401
[41] Gunes F *et al* 2011 *Nano* **6** 409–18
[42] Cho H *et al* 2015 *2D Mater.* **2** 014002
[43] Shin H-J *et al* 2009 *Adv. Funct. Mater.* **19** 1987–92
[44] Hsiao M-C *et al* 2010 *J. Mater. Chem.* **20** 8496–505
[45] Sugiyama K, Ishii H, Ouchi Y and Seki K 2000 *J. Appl. Phys.* **87** 295
[46] Huh S, Park J, Kim Y S, Kim K S, Hong B H and Nam J-M 2011 *ACS Nano* **5** 9799–806
[47] Lee T-W, Chung Y, Kwon O and Park J-J 2007 *Adv. Funct. Mater.* **17** 390–6
[48] Han T-H, Choi M-R, Woo S-H, Min S-Y, Lee C-L and Lee T-W 2012 *Adv. Mater.* **24** 1487–93
[49] Han T-H, Song W and Lee T-W 2015 *ACS Appl. Mater. Interfaces* **7** 3117–25